

Muon-induced fission as a probe of the underlying dynamics in nuclear fission

Christian Ross^{1,*} and A.S. Umar^{1,†}

¹*Department of Physics and Astronomy, Vanderbilt University, Nashville, TN, 37235, USA*

(Dated: July 4, 2025)

Muon-induced fission could be utilized as a probe to study the underlying dynamics of nuclear fission. The probability of muon attachment to the light asymmetric fission fragment is sensitive to fission dynamics, such as the timescale and friction of the fission event, charge asymmetry, and possibly the shape of the fission fragments. We focus on muonic atoms that are formed with actinide nuclei. A relativistic approach is employed, solving the Dirac equation for the muonic wavefunction in the presence of a time-dependent electromagnetic field generated by the fissioning nucleus. Computations are carried out on a 3-D Cartesian lattice with no symmetry assumptions. The results show a strong dependence of the attachment probability on the fission charge asymmetry and a more modest dependence on friction.

Nuclear physics experiments with muon beams provide information on fundamental symmetries and interactions. Muonic atoms, in particular, have proven extremely useful in examining the electromagnetic properties of nuclei, e.g. electric charge distributions and multipole moments, because the muon has a high position probability density inside the nucleus owing to its small Compton wavelength of 1.87 fm. Muonic atoms have been extensively utilized to study nuclear charge radii and quadrupole moments of most stable nuclei [1–6], as well as isotope production through muon capture [6–8]. With recent experimental advances, these studies can now be potentially extended to neutron-rich nuclei. For heavy and neutron-rich nuclei, the muon capture process may be delayed because most neutron levels are occupied. When an actinide nucleus acquires a muon in an excited orbital, the resulting excited muonic atom is also an excellent tool that may be utilized to probe the dynamics of fission. This is largely due to the second-generation lepton possessing a mean lifetime which exceeds typical fission timescales by several orders of magnitude. Muon-induced fission enjoys a rich history of interest from both the experimental community [9–16] and the theoretical community [17–21]. However, most theoretical approaches were either carried out in a non-relativistic framework or employed only crude fission potential models in their studies. With the advent of theoretical static and dynamic fission calculations [22,23] from a microscopic framework, it is desirable to incorporate these into the study of muon-induced fission.

After the formation of an excited muonic atom, the muon cascade of de-excitations begins [24], as depicted in Fig. 1. At higher orbits ($n \approx 14$) the dense level densities could lead to the ejection of Auger electrons, while lower transitions are characterized by x-ray emission. It is important to note the possibility of free decay of the muon

$$\mu^- \longrightarrow e^- + \nu_\mu + \bar{\nu}_e \quad (1)$$

at any point of these processes. Alternatively, it is feasible for the muon to be captured by a proton inside the nucleus

$$(Z, A) + (\mu^-) \longrightarrow (Z-1, A)^* + \nu_\mu \quad (2)$$

which leaves behind a neutron and a muon neutrino. Most of the energy is carried away by the neutrino. The system can de-excite by emitting neutrons and gamma-rays or fissioning during this process. Fission induced in this case is referred to as *delayed* since it occurs on timescales characteristic of the weak decay process' mean lifetime (which occurs on the order $t \approx 10^{-7}$ s). In contrast, prompt fission timescales are shorter than $t \approx 10^{-12}$ s. In Fig. 2 we outline the most common paths

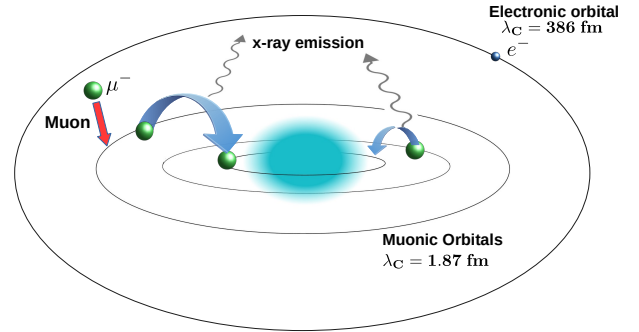


FIG. 1. Depiction of the muon de-excitation process.

an excited muonic atom can take [2,11,25].

Alternatively, as the muon cascades down, inner shell transitions can occur without photon emission through inverse internal conversion

$$(Z, A) + (\mu^-)^* \longrightarrow (Z, A)^* + (\mu^-), \quad (3)$$

in which the transition energy of the muon is directly transferred to the nucleus. In actinide nuclei, the $E1(2p \rightarrow 1s, 6.6 \text{ MeV})$ and $E2(3d \rightarrow 1s, 9.5 \text{ MeV})$ muonic transitions can excite the nuclear giant dipole and giant quadrupole resonances, respectively. These resonances serve as doorway states that facilitate the onset of fission. An inverse internal conversion process also has the potential to excite the nucleus into a metastable isomeric state, leading to isomeric fission. The probability of the muon attaching to the light fission fragment is sensitive to the amount of nuclear friction experienced between the outer fission barrier and the scission point. If friction is high during the evolution from the outer barrier to scission, the muon tends to remain in the lowest molecular orbital, the $1s\sigma$ state, and consequently emerges bound in the $1s$ state

* christian.ross@vanderbilt.edu

† sait.a.umar@vanderbilt.edu

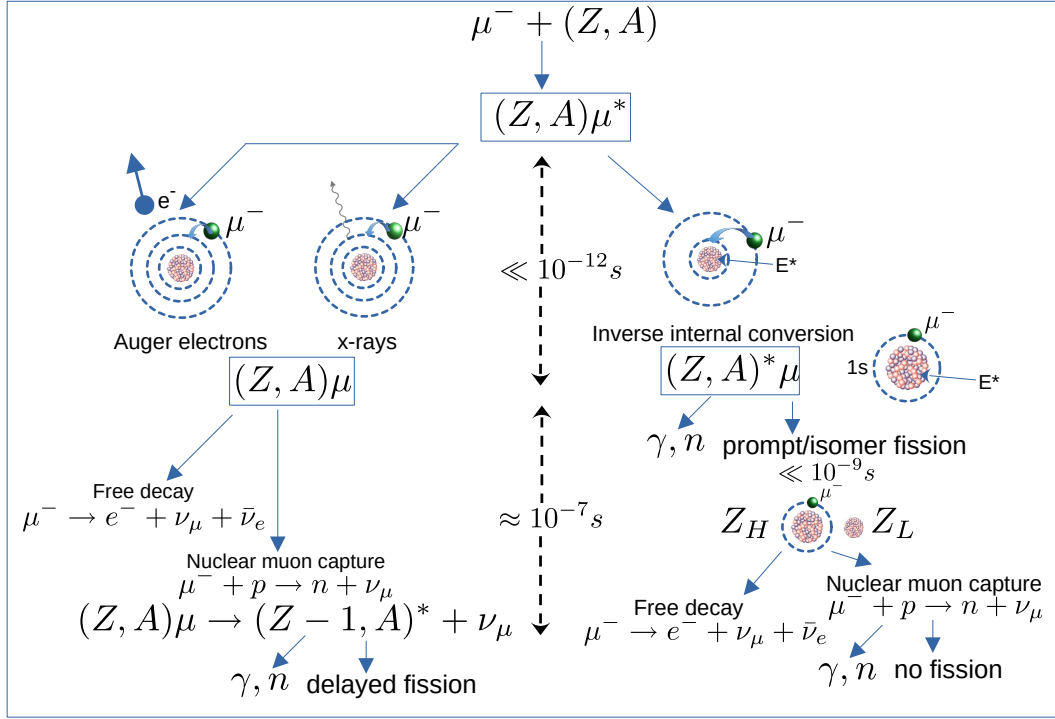


FIG. 2. Possible paths a muonic atom can follow. For detailed description please see the text.

of the heavy fission fragment. Conversely, if nuclear friction is small, allowing for a relatively rapid collective motion, there is a finite probability that the muon may be excited to higher-lying molecular orbitals, such as the $2p\sigma$ state, from which it can ultimately become attached to the light fission fragment. Therefore, theoretical predictions of the probability of attachment of muon to the light fragment, when combined with experimental observations, provide valuable insight into the fission dynamics and, in particular, the mechanisms of nuclear energy dissipation. Other possibilities include back-tunneling, which describes the process of tunneling back from an isomeric state excitation rather than tunneling out to fission and also results in delayed fission. Experimentally, when data are collected by observing muonic x-rays throughout the fission process, prompt and delayed fission modes are distinguished due to their different timescales [12]. Ultimately, the muon would either undergo free-decay or will be captured by one of the fission fragments.

Since the nuclear excitation energy in muon-induced fission is larger than the height of the fission barrier, the fission dynamics can be reasonably treated within a classical framework, without the need to consider quantum tunneling through the barrier. For simplicity, the evolution of the fission process is described using a single collective coordinate, R , representing the separation between the fragments. In this classical picture, the collective nuclear energy takes the form:

$$E_{nuc} = \frac{1}{2}B(R)\dot{R}^2 + V_{fis}(R) + E_{\mu}(R) \quad (4)$$

where a coordinate-dependent mass $B(R)$ is introduced [26]. As the nucleus moves from the outer fission barrier to the scis-

sion point one can also introduce a dissipation term, which depends quadratically on the relative velocity

$$\frac{dE_{nuc}}{dt} = -\frac{dE_{diss}}{dt} = -f\dot{R}^2(t). \quad (5)$$

This constant parameter, f , can be determined from the time-dependent Hartree-Fock (TDHF) evolution [27], but in general can be time-dependent [28]. Equation (5) together with Eq. (4) determines the equation for the collective dynamics to be solved, subject to the initial condition that the kinetic energy contains the excitation energy, $E^* = 9.5$ MeV, corresponding to the $3d \rightarrow 1s$ transition with inverse internal conversion.

The calculation of the fission potential, $V_{fis}(R)$, proceeds in two steps, we first perform constrained Hartree-Fock (CHF) calculations of the fission potential by constraining the quadrupole moment of the nucleus in a standard manner, described for our case in Ref. [29]. Starting from a point after the saddle point we evolve the system using TDHF equations [30] to a large R value (about 80-100 fm). During this evolution we use the density constrained time-dependent Hartree-Fock (DC-TDHF) calculations to obtain the $V_{fis}(R)$ values.

In describing the dynamical evolution of the muonic wavefunction during prompt fission, the dominant interaction arises from the electromagnetic coupling between the muon and the nucleus, characterized by the term $-e\gamma_{\mu}A^{\mu}$. The contribution from the weak interaction is negligible in this context. Furthermore, since the motion of the fission fragments is nonrelativistic, the electromagnetic interaction is primarily governed by the Coulomb force. The muon is a relativistic entity (in the ground state of an actinide muonic atom, the muonic bind-

ing energy is approximately 12% of the muonic rest mass), which strongly implies that calculations performed with the Schrödinger equation are quite limited (note that some groups have shown that this is feasible [31]). Instead, we solve the Dirac equation for the muon in the presence of a time-dependent electromagnetic field generated by the fissioning nucleus. The Dirac equation for a muonic spinor wavefunction in the presence of an external electromagnetic field is given through the minimal coupling prescription

$$\left(i\hbar c \gamma^\mu \partial_\mu - q \gamma^\mu A_\mu(\mathbf{r}, t) - mc^2 \right) \psi(\mathbf{r}, t) = 0. \quad (6)$$

Assuming that the motion of the fission fragments is nonrelativistic, the Coulomb interaction will dominate. The scalar Coulomb potential $A_0(\mathbf{r}, t)$ is several orders of magnitude larger than the vector potential $\mathbf{A}(\mathbf{r}, t)$ components of the electromagnetic four-potential so the vector potential is neglected. The Dirac Hamiltonian can be written as

$$\hat{H}_D = -i\hbar c \alpha^i \partial_i + \beta mc^2 - q A_0(\mathbf{r}, t), \quad (7)$$

with the scalar Coulomb potential obtained by using the proton densities from CHF and TDHF calculations and employing fast Fourier transform (FFT) techniques for the Poisson equation

$$\nabla^2 A_0(\mathbf{r}, t) = -4\pi q^2 \rho_p(\mathbf{r}, t). \quad (8)$$

The solution of the Dirac equation proceeds in two steps: first, a static solution is generated by solving the stationary Dirac equation for the ground-state spinor

$$\hat{H}_D(\mathbf{r}, 0) \psi_{gs}(\mathbf{r}) = E_{gs} \psi_{gs}(\mathbf{r}). \quad (9)$$

Once a static ground-state solution is found, the time-dependent Dirac equation

$$\hat{H}_D \psi(\mathbf{r}, t) = i\hbar \frac{\partial}{\partial t} \psi(\mathbf{r}, t), \quad (10)$$

is propagated in time via a Taylor expansion of the unitary time-evolution operator

$$\psi(t + \Delta t) \approx \left(\mathbb{I} + \sum_{n=1}^N \frac{(-i\Delta t \hat{H}_D)^n}{n!} \right) \psi(t), \quad (11)$$

with $\psi(\mathbf{r}, t=0) = \psi_{gs}(\mathbf{r})$. The instantaneous muonic binding energy E_μ , to be used in Eqs (4) and (5), is given by

$$E_\mu(R(t)) = \langle \psi(\mathbf{r}, t) | \hat{H}_D | \psi(\mathbf{r}, t) \rangle. \quad (12)$$

We have written a new code to solve the Dirac equation on a three-dimensional Cartesian lattice with no symmetry assumptions using the basis-spline discretization [32] method. The static muon wave functions are obtained using the relativistic version of the gradient iteration method [33]. For the three systems studied here, ^{240}Pu , $^{256,258}\text{Fm}$, we vary the quadrupole moment from the ground-state value up to

7400–8000 fm² in steps of 100 fm² and a CHF with Bardeen-Cooper-Schrieffer (BCS) pairing calculation is performed at each constraint step, using the SLy4d Skyrme interaction [34], with a density dependent delta interaction (DDDI) in the pairing channel using neutron and proton strengths 1256 MeV fm³ and 1462 MeV fm³, respectively. The fission potential for ^{240}Pu is doubled humped as shown in Ref. [29], with an inner barrier height of 6.0 MeV and outer barrier height of 3.9 MeV. Whereas the $^{256,258}\text{Fm}$ potentials are single humped [35], with barrier heights of 6.0 and 5.5 MeV, respectively. Past this point, the DC-TDHF dynamic run evolves the system through the remainder of the fission process. CHF and DC-TDHF calculations were performed on a numerical mesh of size $140 \times 32 \times 32$ fm³. The proton densities are then placed on a larger mesh of size $140 \times 70 \times 70$ fm³ for the muon fission code. This is required since the muonic wavefunction spreads out over a relatively large volume. The muon attachment probability is determined by integrating the muon density to the left and right halves of the 3D numerical box, as

$$\begin{aligned} P_L(t) &= \int d^3x \psi^\dagger(\mathbf{x}, t) \psi(\mathbf{x}, t) ; x < 0 \\ P_R(t) &= \int d^3x \psi^\dagger(\mathbf{x}, t) \psi(\mathbf{x}, t) ; x > 0, \end{aligned} \quad (13)$$

satisfying $P_L + P_R = 1$.

As we have mentioned above, the muon attachment probability to the fission fragments is sensitive to fission dynamics and the charge asymmetry of the fragments. ^{240}Pu fissions with a charge asymmetry of $Z_H/Z_L = 1.29$. ^{258}Fm and ^{256}Fm have bimodal fission modes, for ^{258}Fm the symmetric fission mode is more favorable, while for ^{256}Fm the asymmetric mode appears to be favorable [36]. For ^{258}Fm we chose the symmetric fission path, and for ^{256}Fm we chose a path with charge asymmetry of 1.15, corresponding to the heavy fragment having $Z = 54$. Sometimes the additional contribution from muon energy in Eq. (4) has been interpreted as modifying the original fission potential, in our case the modification of the fission barriers due to the muon energy for ^{240}Pu are 0.19 MeV and 0.98 MeV at the inner and outer barriers, respectively. For ^{256}Fm and ^{258}Fm nuclei these modifications are 0.24 MeV and 0.33 MeV, respectively.

TABLE I. Results for ^{240}Pu , ^{256}Fm , and ^{258}Fm systems. For details see text.

| System | ^{240}Pu | ^{256}Fm | ^{258}Fm |
|---------------------|-------------------|-------------------|-------------------|
| Charge asymmetry | 1.29 | 1.15 | 1.0 |
| Mass asymmetry | 1.30 | 1.16 | 1.0 |
| P_L (no friction) | 5.2% | 20.6% | 50.0% |
| f (MeV/fm-c) | 456 | 550 | 562 |
| E_{diss} (MeV) | 21.94 | 29.60 | 18.41 |
| P_L (friction) | 6.5% | 16.6% | 50.0% |

In Table I we show the summary of results at the final asymptotic time-step for the three systems. We note that charge asymmetries are about the same as their mass asymmetries, A_H/A_L , for these systems. We see a strong dependence of the probability of attachment of muons to the light fragment, P_L , on this asymmetry. For the plutonium case with a

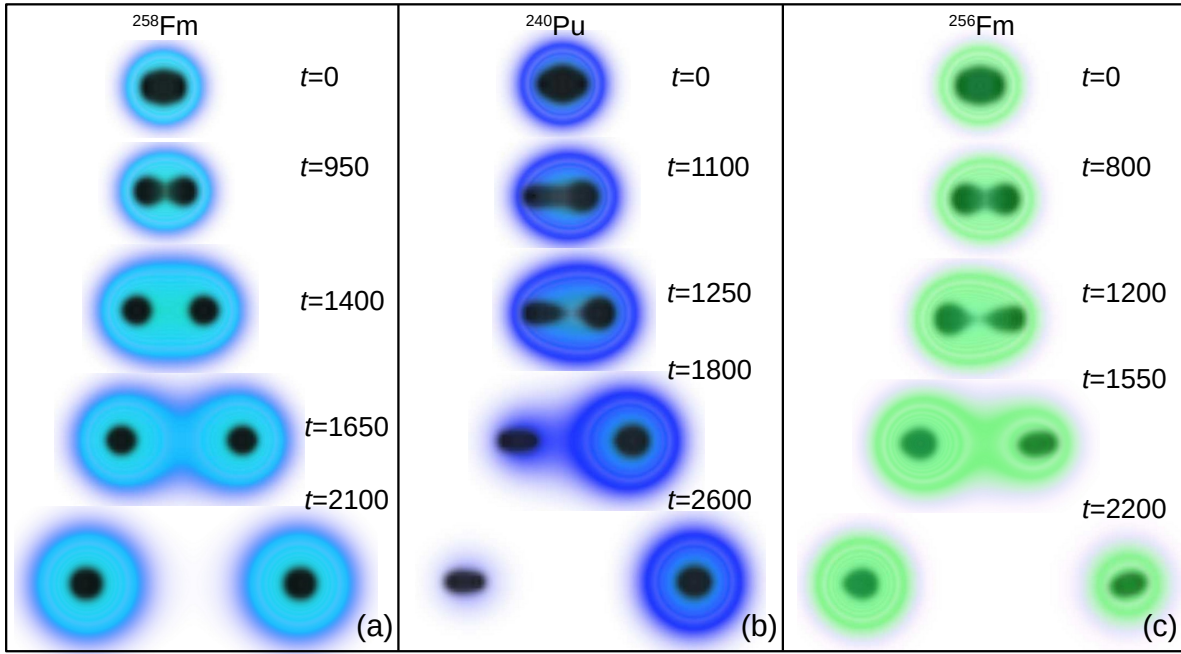


FIG. 3. Time-evolution of the muon density (a) ^{258}Fm : charge asymmetry of 1.0, (b) ^{240}Pu : charge asymmetry of 1.29, (c) ^{256}Fm : charge asymmetry of 1.15. Times are given in units of fm/c. The dark shaded region depicts the nuclear fragment densities.

mass asymmetry of 1.30, this probability is 5.2%, whereas for the ^{256}Fm case with asymmetry value of 1.16 the probability is 20.6%. For the symmetric fission of ^{258}Fm , the muonic wavefunction is evenly split, and the probability is exactly 50%, which also serves as a computational test case. For these cases, when friction is included, these probabilities change to 6.5%, 16.6%, and again 50%. The increase of the light fragment attachment probability in the case of ^{240}Pu from 5.2% to 6.5% does not fit the expectation that with increasing friction this probability should decrease. We have further tested this by artificially increasing the friction parameter and observed that the probability slowly decreases to 0% in the adiabatic limit. Thus we interpret this being a result of the sensitivity of the model to the constant friction model parameter f . The trend for the dissipated energy is similar as well, with the results being commensurate with those given in [27]. Figure 3 shows the time-evolution snapshots of the muon density for (a) ^{258}Fm , (b) ^{240}Pu , and (c) ^{256}Fm , starting from the ground state to the final separation distance of about 100 fm. The dark shaded region depicts the nuclear fragment densities.

Employing a muon as a probe of the underlying dynamics involved in nuclear fission is a promising tool. Due to the sensitivity of the muon attachment probability to the fission fragments, insight can be gained into several physical mechanisms, such as the nuclear dissipation energy and the fission

timescales. We have written a new code to solve the Dirac equation for a muonic spinor wavefunction in the presence of an external time-dependent electromagnetic field generated by the fissioning nucleus. CHF and DC-TDHF calculations were used to generate fission potentials, proton densities, and Coulomb potentials for fissioning systems, ^{240}Pu , ^{256}Fm , and ^{258}Fm . The results show a strong dependence of the muon attachment probability to the light fragment on the fragment charge and mass asymmetry. The dependence on friction, as was modeled in our study, was more modest. There is still the question whether the muon prefers the spherical fragment more compared to the deformed one, which requires more systematic studies. Our long-term goal is to interface our muon code with more sophisticated fission codes and models. In principle, the collective motion of the fissioning nucleus can be integrated with dynamical microscopic fission calculations as was done in Ref. [28,37], which also allows for a time-dependent friction calculation.

ACKNOWLEDGMENTS

This work has been supported by the U.S. Department of Energy under award number DE-SC0013847 (Vanderbilt University).

[1] H. D. Wohlfahrt, E. B. Shera, M. V. Hoehn, Y. Yamazaki, and R. M. Steffen, Nuclear charge distributions in $1f_{7/2}$ -shell nu-

clei from muonic x-ray measurements, *Phys. Rev. C* **23**, 533 (1981).

- [2] D. F. Measday, The nuclear physics of muon capture, *Phys. Rep.* **354**, 243 (2001).
- [3] J. Caparthy, *Muons: New Research* (Nova Science, 2004).
- [4] I. Angeli and K. P. Marinova, Table of experimental nuclear ground state charge radii: An update, *At. Data Nucl. Data Tables* **99**, 69 (2013).
- [5] A. Knecht, A. Skawran, and S. M. Vogiatzi, Study of nuclear properties with muonic atoms, *Eur. Phys. J. Plus* **135**, 777 (2020).
- [6] T. Y. Saito, M. Niikura, T. Matsuzaki, H. Sakurai, M. Igashira, H. Imao, K. Ishida, T. Katabuchi, Y. Kawashima, M. K. Kubo, Y. Miyake, Y. Mori, K. Ninomiya, A. Sato, K. Shimomura, P. Strasser, A. Taniguchi, D. Tomono, and Y. Watanabe, Muonic x-ray measurement for the nuclear charge distribution: The case of stable palladium isotopes, *Phys. Rev. C* **111**, 034313 (2025).
- [7] M. Ciccarelli, F. Minato, and T. Naito, Theoretical study of Nb isotope productions by muon capture reaction on ^{100}Mo , *Phys. Rev. C* **102**, 034306 (2020).
- [8] M. Niikura, T. Y. Saito, T. Matsuzaki, K. Ishida, and A. Hillier, Measurement of the production branching ratios following nuclear muon capture for palladium isotopes using the in-beam activation method, *Phys. Rev. C* **109**, 014328 (2024).
- [9] B. Budick, S. C. Cheng, E. R. Macagno, A. M. Rushton, and C. S. Wu, Muon- and Pion-Induced Fission of Uranium Isotopes, *Phys. Rev. Lett.* **24**, 604 (1970).
- [10] D. Chultem, V. Cojocaru, D. Gansorig, Kim Si Chwan, T. Krogulski, V. D. Kuznetsov, H. G. Ortlepp, S. M. Polikanov, B. M. Sabirov, U. Schmidt, and W. Wagner, Fission of ^{232}Th , ^{238}U and ^{235}U induced by negative muons, *Nucl. Phys. A* **247**, 452 (1975).
- [11] W. W. Wilcke, M. W. Johnson, W. U. Schröder, J. R. Huizenga, and D. G. Perry, Neutron emission from actinide muonic atoms, *Phys. Rev. C* **18**, 1452 (1978).
- [12] W. U. Schröder, W. W. Wilcke, M. W. Johnson, D. Hilscher, J. R. Huizenga, J. C. Browne, and D. G. Perry, Evidence for Atomic Muon Capture by Fragments from Prompt Fission of Muonic ^{237}Np , ^{239}Pu , and ^{242}Pu , *Phys. Rev. Lett.* **43**, 672 (1979).
- [13] D. Ganzorig, P. G. Hansen, T. Johansson, B. Jonson, J. Konijn, T. Krogulski, S. M. Polikanov, G. Tibell, and L. Westgaard, Fission of ^{232}Th and ^{238}U in the interaction with negative muons, *Nucl. Phys. A* **350**, 278 (1980).
- [14] T. Johansson, J. Konijn, T. Krogulski, S. Polikanov, H. W. Reist, and G. Tibell, Muon induced quadrupole photofission, *Phys. Lett. B* **97**, 29 (1980).
- [15] W. W. Wilcke, M. W. Johnson, W. U. Schröder, D. Hilscher, J. R. Birkelund, J. R. Huizenga, J. C. Browne, and D. G. Perry, Actinide muonic atom lifetimes deduced from muon-induced fission, *Phys. Rev. C* **21**, 2019 (1980).
- [16] F. Risse, W. Bertl, P. David, H. Hänscheid, E. Hermes, J. Konijn, C. T. A. M. de Laat, H. Pruys, C. Rösel, W. Schrieder, A. Taal, and D. Vermeulen, Muon attachment in prompt fission of ^{237}Np , *Z. Phys. A* **339**, 427 (1991).
- [17] J. Hadermann and K. Junker, Muon induced fission, *Nucl. Phys. A* **256**, 521 (1976).
- [18] J. A. Maruhn, V. E. Oberacker, and V. Maruhn-Rezwani, Muon-Induced Fission as a Probe for Fission Dynamics, *Phys. Rev. Lett.* **44**, 1576 (1980).
- [19] A. H. Blin and G. Wolschin, Muon-induced prompt fission of uranium, *Phys. Lett. B* **112**, 113 (1982).
- [20] V. E. Oberacker, A. S. Umar, J. C. Wells, M. R. Strayer, and C. Bottcher, Study of nuclear dissipation via muon-induced fission: A relativistic lattice calculation, *Phys. Lett. B* **293**, 270 (1992).
- [21] F. F. Karpeshin, The complex trajectory method in muon-induced prompt fission, *J. Phys. G: Nucl. Part. Phys.* **30**, 1 (2004).
- [22] N. Schunck and L. M. Robledo, Microscopic theory of nuclear fission: a review, *Rep. Prog. Phys.* **79**, 116301 (2016).
- [23] M. Bender, R. Bernard, G. Bertsch, S. Chiba, J. J. Dobaczewski, N. Dubray, S. Giuliani, K. Hagino, D. Lacroix, Z. Li, P. Magierski, J. Maruhn, W. Nazarewicz, J. Pei, S. Péru-Desenfans, N. Pillet, J. Randrup, D. Regnier, P.-G. Reinhard, L. M. Robledo, W. Ryssens, J. Sadhukhan, G. Scamps, N. Schunck, C. Simenel, J. Skalski, I. Stetcu, P. Stevenson, A. S. Umar, M. Verriere, D. Vretenar, M. Warda, and S. Åberg, Future of Nuclear Fission Theory, *J. Phys. G: Nucl. Part. Phys.* **47**, 113002 (2020).
- [24] E. Borie and G. A. Rinker, The energy levels of muonic atoms, *Rev. Mod. Phys.* **54**, 67 (1982).
- [25] Adamczak, A., Antognini, A., Berger, N., Cocolios, T. E., Deokar, N., Düllmann, Ch. E., Eggenberger, A., Eichler, R., Heines, M., Hess, H., Indelicato, P., Kirch, K., Knecht, A., Krauth, J. J., Nuber, J., Ouf, A., Papa, A., Pohl, R., Rapisarda, E., Reiter, P., Ritjoh, N., Roccia, S., Seidlitz, M., Severijns, N., von Schoeler, K., Skawran, A., Vogiatzi, S. M., Warr, N., and Wauters, F., Muonic atom spectroscopy with microgram target material, *Eur. Phys. J. A* **59**, 15 (2023).
- [26] V. E. Oberacker, A. S. Umar, J. C. Wells, C. Bottcher, M. R. Strayer, and J. A. Maruhn, Muon-induced fission: A probe for nuclear dissipation and fission dynamics, *Phys. Rev. C* **48**, 1297 (1993).
- [27] Y. Iwata and T. Nishikawa, Inertial energy dissipation in nuclear dynamics, *Phys. Rev. C* **105**, 044603 (2022).
- [28] Y. Qiang and J. C. Pei, Energy and pairing dependence of dissipation in real-time fission dynamics, *Phys. Rev. C* **104**, 054604 (2021).
- [29] K. Godbey, C. Ross, and A. S. Umar, Isospin composition of fission barriers, *Phys. Rev. C* **110**, L041601 (2024).
- [30] C. Simenel and A. S. Umar, Heavy-ion collisions and fission dynamics with the time-dependent Hartree-Fock theory and its extensions, *Prog. Part. Nucl. Phys.* **103**, 19 (2018).
- [31] V. E. Oberacker, A. S. Umar, and F. F. Karpeshin, Prompt muon-induced fission: A sensitive probe for nuclear energy dissipation and fission dynamics, in *Muons: New Research* (Nova Science, 2004) pp. 179–207, edited by J. Caparthy.
- [32] A. S. Umar, J. Wu, M. R. Strayer, and C. Bottcher, Basis-spline collocation method for the lattice solution of boundary-value problems, *J. Comp. Phys.* **93**, 426 (1991).
- [33] C. Bottcher, M. R. Strayer, A. S. Umar, and P.-G. Reinhard, Damped relaxation techniques to calculate relativistic bound-states, *Phys. Rev. A* **40**, 4182 (1989).
- [34] Ka-Hae Kim, Takaharu Otsuka, and Paul Bonche, Three-dimensional TDHF calculations for reactions of unstable nuclei, *J. Phys. G: Nucl. Part. Phys.* **23**, 1267 (1997).
- [35] G. Scamps, C. Simenel, and D. Lacroix, Superfluid dynamics of ^{258}Fm fission, *Phys. Rev. C* **92**, 011602(R) (2015).
- [36] A. Staszczak, J. Dobaczewski, and W. Nazarewicz, Bimodal fission in the Skyrme-Hartree-Fock approach, *Acta Phys. Pol. B* **38**, 1589 (2007).
- [37] Y. Qiang, J. C. Pei, and P. D. Stevenson, Fission dynamics of compound nuclei: Pairing versus fluctuations, *Phys. Rev. C* **103**, L031304 (2021).